Journal of Power Sources 206 (2012) 77–83

Contents lists available at SciVerse ScienceDirect

Journal of Power Sources

journal homepage: www.elsevier.com/locate/jpowsour

A composite sol–gel process to prepare a YSZ electrolyte for Solid Oxide Fuel Cells

E. Courtin[a,*], P. Boy[a], T. Piquero[b], J. Vulliet[b], N. Poirot[c], C. Laberty-Robert[d]

[a] CEA/DAM Le Ripault, Laboratoire Sol–Gel et Simulation, 37260 Monts, France
[b] CEA/DAM Le Ripault, Laboratoire Céramiques et Composants Avancés, 37260 Monts, France
[c] Laboratoire d'Electrodynamique des Matériaux Avancés-UMR 6157, Université de Tours, IUT de Blois, 15 rue de la Chocolaterie, C.S. 2903, 41000 Blois, France
[d] Laboratoire de Chimie de la Matière Condensée de Paris, Collège de France, 11 place Marcelin-Berthelot, 75231 Paris Cedex 05, France

ARTICLE INFO

Article history:
Received 22 November 2011
Received in revised form 12 January 2012
Accepted 15 January 2012
Available online 25 January 2012

Keywords:
Solid Oxide Fuel Cells
Sol–gel
Electrolyte
YSZ

ABSTRACT

ZrO_2–8% Y_2O_3 (YSZ) thick film was deposited on a YSZ–NiO anode and co-sintered to obtain a gas-tight electrolyte for an application as Solid Oxide Fuel Cell. A YSZ sol–gel composite sol is synthesized from a YSZ colloidal binder and a YSZ commercial powder and deposited as a thick (>10 μm) monolayer by the dip-coating process. The evolution of the composite sol viscosity with time and its influence on the deposited film thickness is studied. The influence of the composite sol composition, the film sintering on the films microstructure is also studied in order to achieve dense films. The interest of co-sintering the electrolyte with the anodic support is demonstrated. Ionic conductivity and activation energy are measured on pellets obtained from pressed-powder obtained from (a) the calcination of composite sol and (b) the commercial powder. Conductivity of 0.03 S cm^{-1} at 800 °C and activation energy of 0.9 eV were measured through impedance spectroscopy. Finally, an entire cell is processed with the developed electrolyte and polarization curves (I–V) were measured at 850 °C. OCV of 1.23 V was achieved, indicating the quality of the synthesized YSZ electrolyte.

1. Introduction

Solid Oxide Fuel Cells (SOFC) are of particular interest due to their high energy conversion efficiency, low pollution emission and ability to work with various fuels [1].

Yttria-stabilized zirconia (ZrO_2–8 mol.% Y_2O_3) is the most widely used material for electrolyte because of its high ionic conductivity, good chemical and mechanical stability[2]. SOFCs with an electrolyte support usually work at high temperatures (1000 °C) which leads to a fast degradation of the stack and the use of expensive interconnect materials [1,3]. In order to decrease this operating temperature to 800 °C, either new electrolyte materials have to be processed, or the electrolyte thickness has to be decreased in order to reduce the ohmic loss [4,5]. It is generally admitted that 10 μm thick electrolyte is a good compromise between low ohmic losses and good mechanical strength [6]. Such a thin electrolyte is then deposited on an anode support. Processing a gas tight electrolyte is one of the main challenges of this configuration.

Sol–gel chemistry has many advantages to process YSZ electrolytes such as low cost, a good control of solution homogeneity, a good film thickness control and possibly low processing temperatures. Furthermore, it allows deposition on non-planar anodic supports using the dip-coating technique [7]. A good control of the sol viscosity is necessary when using the dip-coating technique to process a film in the appropriate thickness range. The main limitation in sol–gel process is the difficulty to process crack free films thicker than 1 μm. Indeed, due to mechanical stress during drying, ceramic films up to 0.5 μm are deposited in a single layer. Thicker films are achieved by depositing multiple layers [8]. To achieve a thickness of around 10 μm in one layer, a composite sol, first developed by Barrow et al. [8] for lead zirconate titanate (PZT) piezo-electric films, can be used. It consists in mixing a YSZ sol with YSZ powders to increase the deposited thickness. The YSZ sol is a hydro-alcoholic solution containing stabilized yttrium and zirconium precursors. Barrow et al. [9] explained interactions between the sol and the powder: the sol behaves as a mortar surrounding the ceramic particles as bricks in a wall. Films do not crack during the process, probably because a strongly bonded network is formed with the sol–gel binder between ceramic particles.

A homogeneous crack-free film is more difficult to achieve with an organic binder using dip-coating because high porosities are created during their decomposition. Then, densification is difficult to achieve even after high heat-treatment because stable porosity is formed. To our knowledge, very few studies report the deposition of YSZ suspensions in organic media using the dip-coating process. Xia et al. [10] described dispersion of YSZ powders in ethanol deposited on porous substrate by dip-coating. However, films exhibit low

* Corresponding author. Tel.: +33 247344302.
E-mail addresses: emiliecourtin@gmail.com (E. Courtin), philippe.boy@cea.fr (P. Boy), thierry.piquero@cea.fr (T. Piquero), julien.vulliet@cea.fr (J. Vulliet), nathalie.poirot@univ-tours.fr (N. Poirot), christel.laberty@upmc.fr (C. Laberty-Robert).

0378-7753/$ – see front matter © 2012 Elsevier B.V. All rights reserved.
doi:10.1016/j.jpowsour.2012.01.109

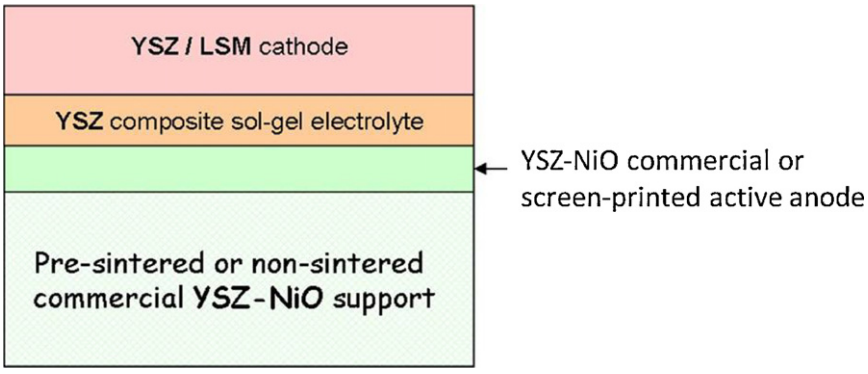

Fig. 1. Composition of the tested cell.

thickness and cracks. Gaudon et al. [11] described the realization of porous films on dense and porous substrates by dip-coating YSZ suspensions. These suspensions were prepared by mixing a polymer matrix with a stable suspension of commercial YSZ powders in a methyl ethyl ketone/ethanol azeotropic solvent. Composition of this type of suspension was improved by Lenormand et al. [12] and Viazzi et al. [13] to obtain a higher density of the deposited YSZ layers. These YSZ films were deposited on dense or porous substrates but to our knowledge no electrochemical tests were performed on an entire cell.

In this study, a sol–gel composite process, with a limited organic content, was used to synthesize dense YSZ layers on YSZ–NiO cermets by dip-coating. The influence of sol composition (binder concentration and powder load), thermal treatment and co-sintering were investigated to control films microstructure. Sol ageing was also studied by viscosity measurements. Electrochemical properties were characterized by impedance spectroscopy and an entire cell was processed to measure the electrolyte performances.

2. Experimental

2.1. YSZ sol synthesis

A solution containing yttrium and zirconium precursors was synthesized using the alkoxide route [14]. As colloids are formed in solution, this sol will be called colloïdal sol. The zirconium alkoxide precursor is zirconium (IV) propoxide ($Zr(OPr)_4$), 70 wt% solution in 1-propanol (Aldrich). Acetylacetone (Fluka) is added as a complexing agent to limit the strong reactivity of $Zr(OPr)_4$ with moisture. Yttrium (III) nitrate hexahydrate (Aldrich) dissolved in 1-propanol (Sigma Aldrich) is then added to obtain the ZrO_2–8 mol.% Y_2O_3 sol. HCl (37%, Prolabo) in water is finally added. Hydrolysis rate ($h = [H_2O]/[Zr]$) and complexing ratio ($x = [Acac]/[Zr]$) are, respectively, $h = 2.8$ and $x = 0.8$.

2.2. Composite sol synthesis

The composite sol preparation consists in mixing a commercial YSZ powder (Tosoh) with the YSZ colloidal sol, called binder, 0.5 wt% of Triton X (Aldrich), used as a dispersant, and 5 wt% of ethylene glycol (VWR) to increase the sol viscosity. Powder content and YSZ sol concentration were chosen in order to obtain a single layer in the appropriate thickness range (10–20 μm). Mixtures were stirred under constant agitation for several months to study sol ageing.

2.3. Cell preparation

YSZ layers were deposited on sintered and non-sintered YSZ–NiO commercial anodic support. Pre-sintered supports were

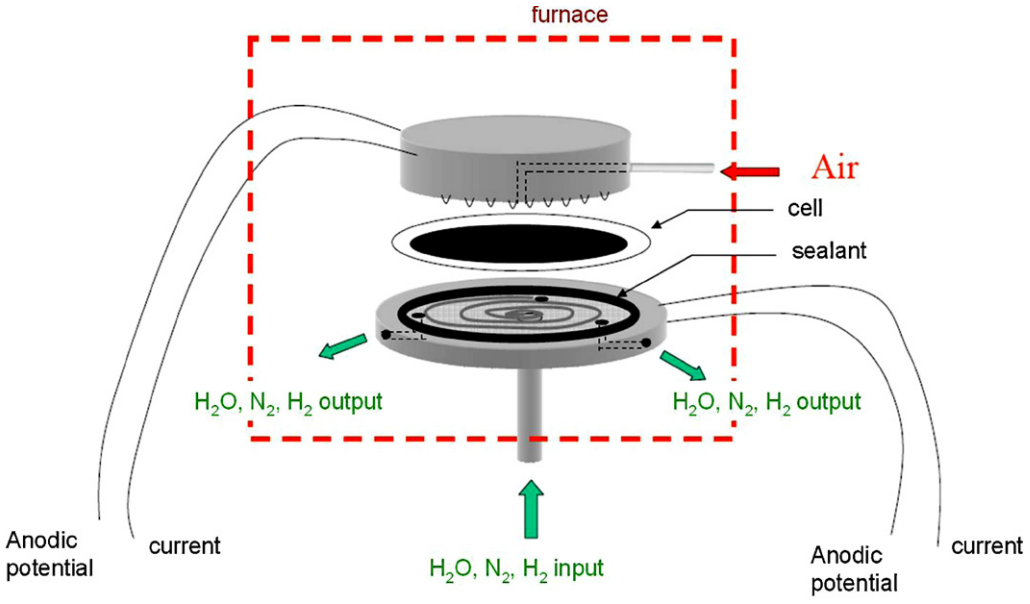

Fig. 2. Test assembly.

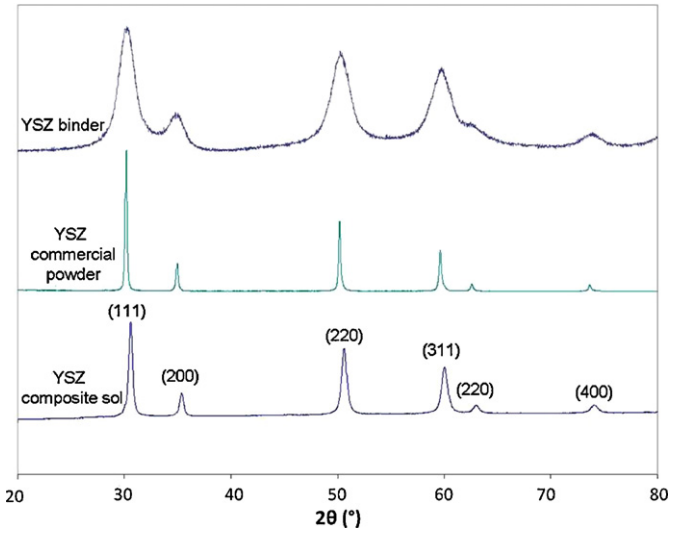

Fig. 3. XRD diffraction patterns of sol–gel YSZ colloïdal sol, YSZ commercial powder and YSZ composite sol.

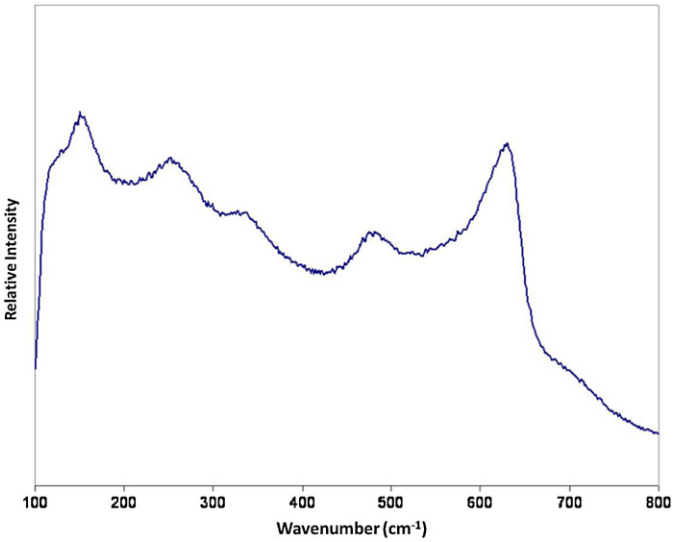

Fig. 4. Raman spectra of the YSZ colloidal sol calcined at 600 °C.

already coated with a commercial YSZ–NiO anode whereas, on non-sintered supports, the anode layer was deposited by screen-printing and dried at 200 °C before depositing the electrolyte. YSZ composite sol was then deposited by dip-coating and heat-treated at 700 °C for 2 h and then up to 1400 °C during 12 h with a heating rate of 120 °C h^{-1}. Finally, a YSZ/LSM layer was screen-printed on the electrolyte to test the entire cell. The cell composition is shown in Fig. 1.

2.4. Characterization

Viscosity measurements were performed with a Haake Rheostress 1 in a cone-plate configuration.

For characterization, sols were dried at 120 °C or calcined at 600 °C during 5 h, with a heating rate of 120 °C h^{-1}. Sols were characterized by simultaneous Differential Thermal Analysis (DTA) and Thermogravimetric Analysis (TGA) using a SETARAM TAG 24 and a 10 °C min^{-1} heating rate. Powders were characterized by X-ray Diffraction (XRD) with a PANALYTICAL X'PERT PRO diffractometer using the Cu Kα1 radiation. The crystallite size was determined by the Debye–Scherrer formula [15].

Raman characterizations were performed with a T64000 Jobin Yvon spectrometer. The chosen excitation laser radiation was the 633 nm line.

Films microstructure was observed by Scanning Electron Microscopy (SEM), using a Hitachi S_2500 and SEM-FEG, S440 LEICA.

Densification kinetics and the final shrinkages of the electrolyte were controlled by dilatometric measurements performed in air at 2 °C min^{-1} up to 1600 °C with a 2 h dwell-time (dilatometer SETSYS Evolution 2400, SETARAM).

To characterize electrical properties by impedance spectroscopy, 20 mm diameter YSZ pellets were prepared by uniaxial pressing the powder with a pressure of 3 tonnes. The compacts were then sintered in air at 1400 °C for 10 h with a 120 °C h^{-1} heating rate. Before pressing, YSZ powders were calcined at 200 °C and 700 °C and milled after each calcination step in a planetary ball milling for 45 min. Electrochemical measurements on symmetrical Platinum (Pt)/YSZ/Pt cells (electrode surface of nearly 3.1 cm^2) were carried on using AC impedance spectroscopy (SOLARTRON 1260). Measurements were performed in static air between 700 °C and 900 °C with a 30–50 mV signal amplitude at open circuit voltage in the 10^{-1} to 10^6 Hz frequency range.

Single cell was installed in an assembly according to Fig. 2. The experimental device allowed a feeding of the cell with water and hydrogen, diluted with nitrogen, on the anodic side and an air supply on cathodic side. The presence of hydrogen caused the reduction of nickel oxide in the cermet during the cell early functioning (nickel in its oxidized state was present in the cell). For

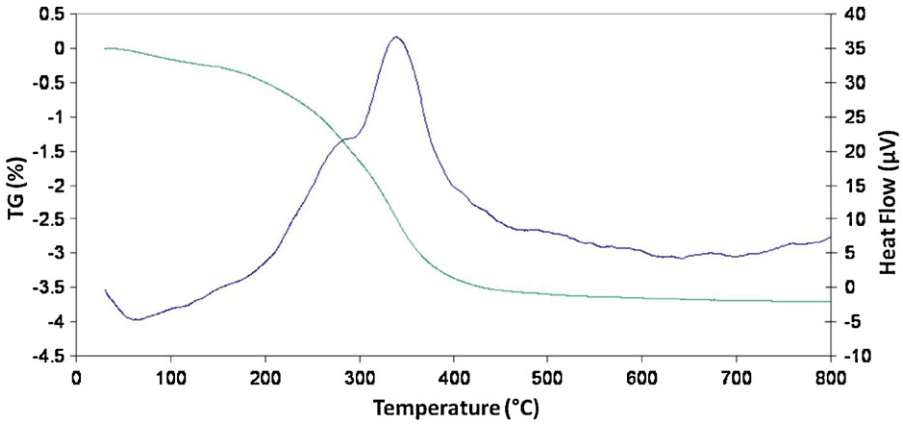

Fig. 5. TDA/TGA performed in air on the composite sol (heating rate: 10 °C min^{-1}).

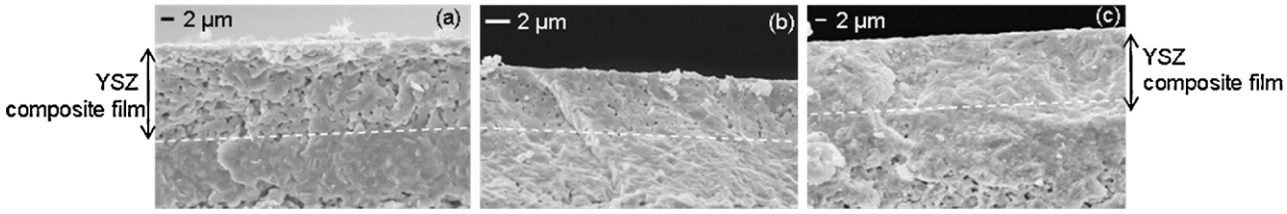

Fig. 6. Evolution of the composite film microstructure with binder concentration (a) $C_l = 0\ mol\ L^{-1}$, $C_p = 60\ wt\%$, (b) $C_l = 0.05\ mol\ L^{-1}$, $C_p = 60\ wt\%$, and (c) $C_l = 0.2\ mol\ L^{-1}$, $C_p = 56\ wt\%$.

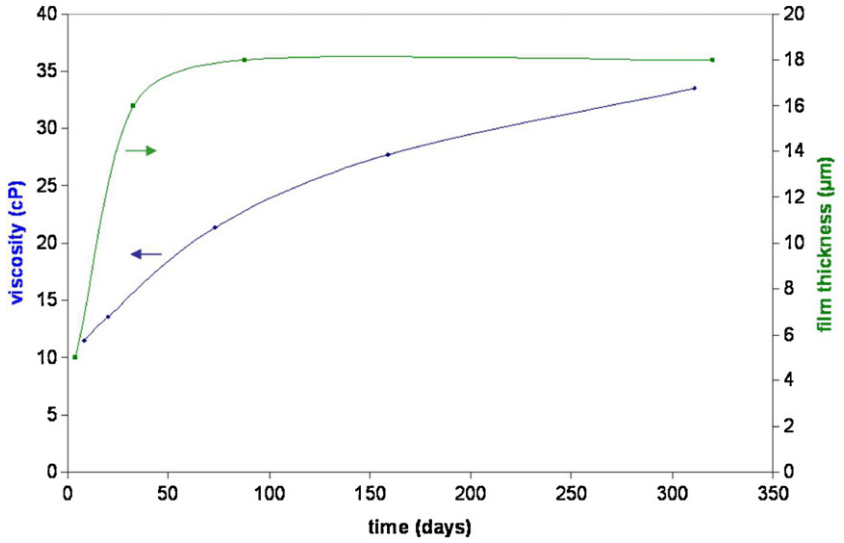

Fig. 7. Evolution of the composite sol viscosity and film thickness with time.

electrical connectors, specific wires, in which there was no current flow, were dedicated to measure the tension. The anodic side was sealed, whereas the cathode output sealing was not ensured since the enhancement of oxygen unused was not under investigation. A load ($200\ g\ cm^{-2}$) was applied to the cell to ensure a proper electrical contact. The system was raised to 850 °C at a rate of $0.5\ °C\ min^{-1}$ under a nitrogen atmosphere. Non-humidified hydrogen was then gradually introduced to ensure the cermet reduction. At first, before the cell characterization as a function of various parameters, a rapid test at 850 °C was performed in order to validate the system (integrity of the cell, full cermet reduction, etc.).

3. Results and discussion

3.1. Composite sol characterization

X-ray Diffraction performed on the YSZ binder dried at 600 °C, the YSZ commercial powder and the composite sol dried at 600 °C are shown in Fig. 3. Cubic phase (*Fm*3*m*), characteristic of ZrO_2–8% Y_2O_3 is obtained for all three materials. The crystallite size was determined with the Debye–Scherrer formula. Crystallites coming from the colloidal sol are 6 nm large whereas Tosoh particles are much larger (100 nm). As YSZ binder crystallites are very thin,

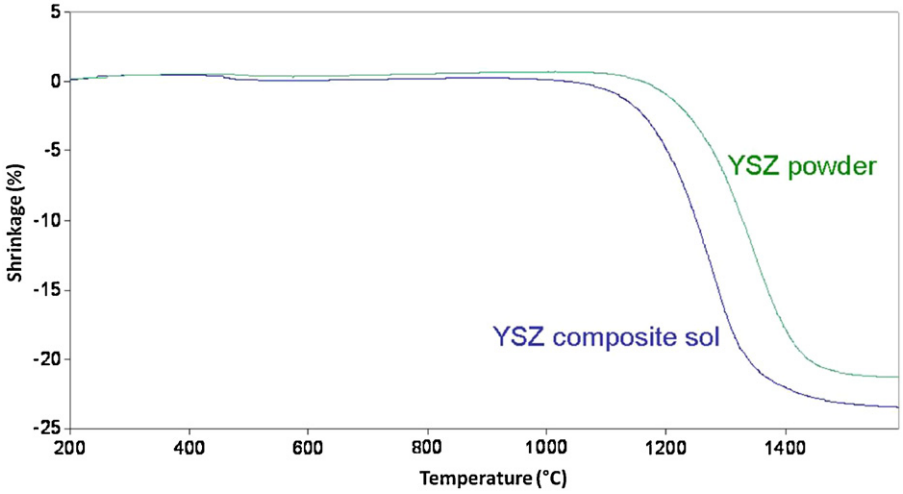

Fig. 8. Dilatometry curves recorded on pellets made of commercial YSZ powder and YSZ composite sol (heating rate: $5\ cm\ min^{-1}$; atmosphere: air).

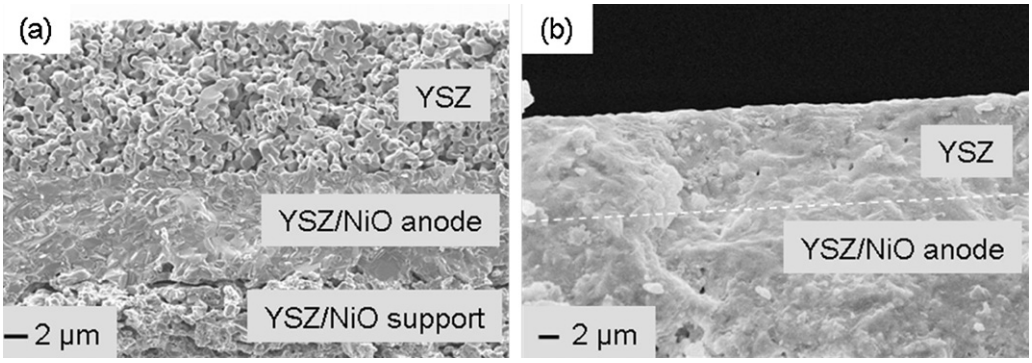

Fig. 9. Evolution of the film microstructure with the sintering temperature (a) 1300 °C and (b) 1400 °C.

deconvolution of the cubic and tetragonal phase could not be achieved by X-ray Diffraction. Raman spectroscopy was performed to identify the crystallites phase (Fig. 4). The result suggests that the binder consists mainly of cubic phase. However, the band at 260 cm^{-1} and 475 cm^{-1} are characteristic bands of the tetragonal phase (*P*42/*nmc*) [16,17] demonstrating powders are crystallized in a mixture of cubic and tetragonal phases.

TG/TD analysis in air was performed on the composite sol dried at 120 °C (Fig. 5). The weight loss of approximately 0.25% from room temperature to 150 °C corresponds to the evaporation of residual free organics (propanol) and water. The exothermic peak at 340 °C is linked to the decomposition of organic species mainly to the departure of bound acetylacetone [18].

From these thermal analyses, a step at 700 °C was performed during heat treatment to make sure that all organics were decomposed before the densification process. This step is essential to limit the porosities formation.

3.2. Influence of the composite sol composition

To observe the influence of the composite sol composition on the film microstructure, composite sols with various colloidal sol concentration (C_I) and powder content (C_P) were deposited on pre-sintered anodic support and then heated up to 1400 °C.

Fig. 6 shows that a very porous layer with open porosities is obtained when Tosoh is dispersed in solvant (propanol) without the addition of the YSZ nanoparticles (C_I = 0 mol L^{-1}). A powder content of 60% was added to obtain a layer thickness of approximately 10 µm. It is also observed that when the colloidal sol concentration increases up to 0.2 mol L^{-1}, film porosity decreases. It confirms that the colloidal sol behaves as a mortar around the commercial particles. Moreover, with a more concentrated binder (0.2 mol L^{-1}), the powder content had to be lowered to 56% to deposit the appropriate layer thickness. With a colloidal sol concentration over 0.2 mol L^{-1}, sols were less stable, films less homogeneous and cracks started to appear. Indeed, when increasing sol binder concentration, powder content had to be decreased to deposit the appropriate thickness. It indicates that a significant amount of ceramic powder (>50%) is necessary to limit cracks during processing because when the percentage of sol–gel in the film is decreased, less shrinkage occurs when the film is processed and so less cracks are formed [9].

On one hand, the sol–gel binder is favourable for the film densification but on the other hand a too concentrated binder generates cracks.

A composite sol made with a 0.2 mol L^{-1} concentrated binder and a powder content of 56 wt% was then chosen as it appeared to be the optimized composition to get a 10 µm thick and dense YSZ layer by dip-coating.

3.3. Composite sol ageing

Composite sol viscosity versus time is plotted in Fig. 7. It shows that viscosity increases with time from 11 cP to 33 cP after 300 days. It can be attributed to a better powder dispersion with time. As layers thickness depends on sol viscosity, according to the Landau and Levich law [19], layers thickness also increases with time, so a wide range of film thicknesses (from 4 to 18 µm) can be achieved using the composite sol–gel process. It can be noted that as viscosity stabilizes, deposited film thickness stabilizes too and a maximum thickness of 18 µm has been obtained. Film thickness can also be controlled by dilution to decrease the sol viscosity.

3.4. Influence of the sintering temperature and the co-sintering on the YSZ film microstructure

Dilatometry measurements were first performed on the Tosoh commercial powder and on the composite sol. Fig. 8 shows that adding the sol–gel YSZ binder slightly decreases the sintering temperature. Indeed Tosoh sintering temperature is estimated at 1350 °C whereas the composite sol sintering temperature is around 1280 °C. Moreover, shrinkage is higher for the composite sol (24%) than for the commercial powder (21%). This is in agreement with the observations made by Zhao et al. [20] describing a best sintering behaviour when two populations of particles are mixed in the sol, which is the case here with YSZ sol–gel crystallites (6 nm) mixed with commercial powder (100 nm).

SEM images in Fig. 9 show that porosity decreases by increasing the sintering temperature from 1300 to 1400 °C. However, for these films deposited on pre-sintered commercial supports, a high

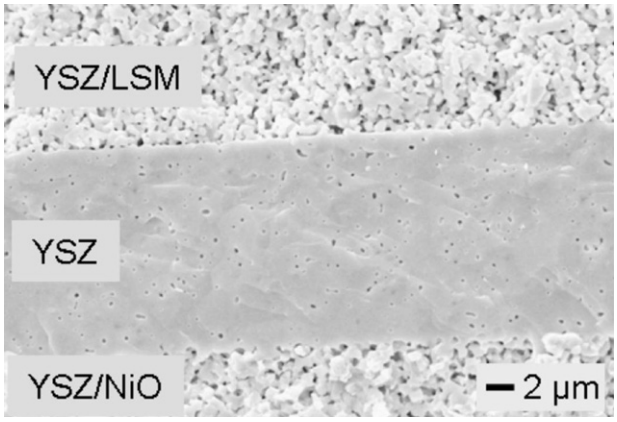

Fig. 10. SEM image, after reduction during cell test, of YSZ electrolyte deposited on a non-sintered support and co-sintered at 1400 °C.

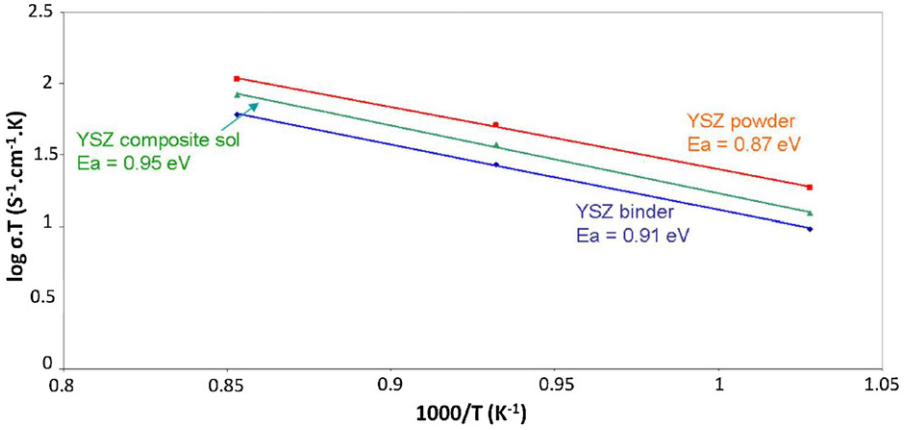

Fig. 11. Arrhenius plots of the conductivity for the YSZ pellets: (a) Tosoh, (b) YSZ binder, and (c) composite sol.

density is very difficult to obtain even at temperatures as high as 1400 °C. Indeed, with pre-sintered supports, stresses due to the difference of Coefficient of Thermal Expansion (CTE) between YSZ electrolyte [21] and sintered YSZ–NiO anode do not allow total densification of the YSZ film. This is the reason why YSZ films were then deposited on non-sintered supports to obtain gas-tight electrolyte by reducing the difference between support and electrolyte CTEs during thermal treatment. Fig. 10 shows a cross-section SEM image of the YSZ composite film deposited on a non-sintered YSZ–NiO anodic support and functional anode layer. The film and the anode were co-sintered at 1400 °C. The 18 μm thick electrolyte is dense with only closed porosities. Cell test on the entire cell has been performed with this electrolyte. The thickness and the density of this electrolyte have been used to perform fuel cell test.

3.5. Electrochemical characterizations

Impedance spectroscopy was performed on pellets made with YSZ commercial powder, binder and composite sol. In Fig. 11, Arrhenius plots for all three materials are plotted. Activation energies for all three materials are close to 1 eV, the usual value for the YSZ ionic conductivity [22], the lowest activation energy being obtained with the YSZ commercial powder (E_a = 0.85 eV). Lowest conductivities are obtained with the YSZ binder but are still comparable to the commercial powder which indicates that the YSZ particles used in the binder exhibit good electrical characteristics with activation energy of 0.91 eV. It can be noted that when added to the commercial powder, they tend to decrease the composite sol conductivity compared to the powder. The composite sol is still 0.03 S cm^{-1} at 800 °C. This value corresponds to expected ZrO_2–8% Y_2O_3 conductivity at 800 °C [23]. This means that this electrolyte material can be used for an intermediate temperature SOFC.

The current–voltage (*I*–*V*) and current–power density (*I*–*P*) of the entire cell made with an YSZ electrolyte (SEM cross-section of the tested cell in Fig. 10) from the developed composite sol is presented in Fig. 12. The Open Circuit Voltage (OCV) is 1.23 V at 850 °C. This value is closed to the theoretical values predicted by the Nernst equation [24], indicating that the electrolyte is dense and there is no gas-leakage. The power density of 350 mW cm^{-2} is obtained in the test conditions (Q_{H2} = Q_{air} = 1.2 NL min^{-1}). However, higher power density will be probably achieved after an optimization of the interface between the electrode and the electrolyte. Further experiments will be devoted to the improvement of the microstructure of the electrode in order to improve the cell performance as it was demonstrated by Virkar et al. [25].

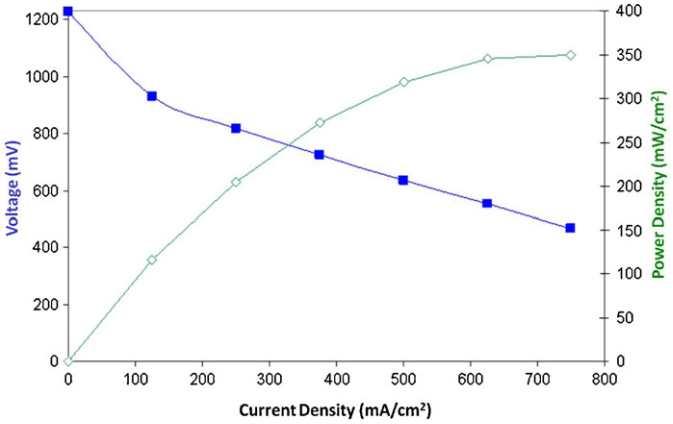

Fig. 12. Voltage and power density for the entire cell, measured at 850 °C. Cell composition: YSZ–NiO anodic support (500 μm), YSZ–NiO functional anodic layer (10 μm), YSZ electrolyte (18 μm), and YSZ/LSM cathode (40 μm).

4. Conclusions

The composite sol–gel process was successfully used to synthesize a dense and gas-tight YSZ electrolyte for an application in Solid Oxide Fuel Cells. The influence of the sol composition on the microstructure was studied leading to an optimal composition. The sol ageing was studied as well as the influence of the sintering temperature. The interest of co-sintering has been demonstrated to obtain dense YSZ film. Finally, electrical characteristics of the composite sol were measured and found to be very similar to the commercial powder. Fuel cell test made on cell made of a YSZ–NiO anode, a YSZ developed electrolyte and a YSZ–LSM cathode was performed. Performance indicate that the electrolyte is gas-tight an OCV of 1.2 V is achieved and a peak power density of 350 mW cm^{-2} at 850 °C.

Acknowledgments

The Region Centre provided financial support for this work. The authors would like to thank V. Frotté (CEA) for TD/TG analysis and the Laboratoire Microstructure et Comportement (CEA).

References

[1] B.C.H. Steele, A. Heinzel, Nature 414 (6861) (2001) 345–352.
[2] S.M. Haile, Acta Materialia 51 (19) (2003) 5981–6000.
[3] K.C. Wincewicz, J.S. Cooper, Journal of Power Sources 140 (2) (2005) 280–296.
[4] P. Charpentier, et al., Solid State Ionics 135 (1–4) (2000) 373–380.

[5] S. de Souza, S.J. Visco, L.C. De Jonghe, Solid State Ionics 98 (1–2) (1997) 57–61.
[6] S.A. Barnett, Energy 15 (1) (1990) 1–9.
[7] C.J. Brinker, G.W. Scherer, Sol–Gel Science: The Physics and Chemistry of Sol–Gel Processing, Academic Press, 1990.
[8] D.A. Barrow, T.E. Petroff, M. Sayer, Surface and Coatings Technology 76–77 (Part 1) (1995) 113–118.
[9] D.A. Barrow, et al., Journal of Applied Physics 81 (2) (1997) 876–881.
[10] C. Xia, et al., Solid State Ionics 133 (3–4) (2000) 287–294.
[11] M. Gaudon, et al., Journal of the European Ceramic Society 26 (15) (2006) 3153–3160.
[12] P. Lenormand, et al., Journal of the European Ceramic Society 25 (12) (2005) 2643–2646.
[13] C. Viazzi, et al., Journal of Power Sources 196 (6) (2011) 2987–2993.
[14] M. Chatry, M. Henry, J. Livage, Materials Research Bulletin 29 (5) (1994) 517–522.
[15] A.L. Patterson, Physical Review 56 (10) (1939) 978.
[16] S. Boulfrad, E. Djurado, J. Fouletier, Solid State Ionics 180 (14–16) (2009) 978–983.
[17] R.R. Piticescu, et al., Journal of the European Ceramic Society 24 (6) (2004) 1941–1944.
[18] S. de Monredon, et al., Journal of Materials Chemistry 12 (8) (2002) 2396–2400.
[19] L.D. Landau, B.G. Levich, Acta Physiochimica URSS 17 (1947) 42–54.
[20] H. Zhao, et al., Journal of Materials Processing Technology 200 (1–3) (2008) 199–204.
[21] K. Haberko, et al., Journal of Power Sources 195 (17) (2010) 5527–5533.
[22] M. Mogensen, et al., Journal of the Electrochemical Society 141 (8) (1994) 2122–2128.
[23] O. Yamamoto, et al., Solid State Ionics 79 (1995) 137–142.
[24] J. Larminie, A. Dicks, Fuel Cell Systems Explained, John Wiley and Sons Ltd., 2003.
[25] A.V. Virkar, et al., Solid State Ionics 131 (1–2) (2000) 189–198.